Long-time-scale dynamics of spin textures in a degenerate F=1 ^{87}Rb spinor Bose gas

J. Guzman, G.-B. Jo, A. N. Wenz, K. W. Murch, C. K. Thomas, and D. M. Stamper-Kurn

Long timescale dynamics of spin textures in a degenerate F=1 ^{87} Rb spinor Bose gas

J. Guzman[1], G.-B. Jo[1], A. N. Wenz[1,3], K. W. Murch[1], C. K. Thomas[1], and D. M. Stamper-Kurn[1,2]

[1]*Department of Physics, University of California, Berkeley CA 94720*
[2]*Materials Sciences Division, Lawrence Berkeley National Laboratory, Berkeley, CA 94720*
[3]*Physikalisches Institut, Ruprecht-Karls-Universität Heidelberg, 69120 Heidelberg, Germany*

We investigate the long-term dynamics of spin textures prepared by cooling unmagnetized spinor gases of $F = 1$ ^{87}Rb to quantum degeneracy, observing domain coarsening and a strong dependence of the equilibration dynamics on the quadratic Zeeman shift q. For small values of $|q|$, the textures arrive at a configuration independent of the initial spin-state composition, characterized by large length-scale spin domains, and the establishment of easy-axis (negative q) or easy-plane (positive q) magnetic anisotropy. For larger $|q|$, equilibration is delayed as the spin-state composition of the degenerate spinor gas remains close to its initial value. These observations support the mean-field equilibrium phase diagram predicted for a ferromagnetic spinor Bose-Einstein condensate, but also illustrate that equilibration is achieved under a narrow range of experimental settings, making the $F = 1$ ^{87}Rb gas more suitable for studies of nonequilibrium quantum dynamics.

Extensive efforts are underway to utilize ultracold atoms as simulators of condensed-matter systems, making use of their broad tunability and amenity to novel experimental probes [1]. The success of these endeavors hinges on the cold-atom system's arriving at equilibrium, matching the conditions of solid state systems that reside at or near the thermal equilibrium state. However, given their limited lifetime, weak interactions, long dynamical timescales, and several nearly conserved quantities, whether equilibrium is reached in cold-atomic materials has become a pressing scientific question [2–4].

One promising system for studying materials physics is the spinor Bose gas, comprised of atoms that may explore all Zeeman states within a spin F manifold. At low temperature, quantum degenerate spinor gases exhibit spontaneous symmetry breaking [5, 6], magnetic order, and intricate spin textures [7, 8] governed by the interplay of magnetism and superfluidity. Several works have examined the ground state of a spatially uniform $F = 1$ spinor gas for which the spin-dependent contact interaction, characterized by a coupling strength $c_2 = 4\pi\hbar^2\Delta a/m < 0$, favors magnetized spin states [9–12]; here Δa is a difference in s-wave scattering lengths, and m is the atomic mass. Under the application of a quadratic Zeeman energy qF_x^2, with F_x being the dimensionless spin projection along an experimentally selected axis $\hat{x}$, and neglecting linear Zeeman shifts, both mean-field and exact many-body treatments predict a symmetry breaking phase transition between paramagnetic and ferromagnetic phases at a positive quadratic Zeeman shift $q = q_0 = 2|c_2|n$ where n is the gas density. Within the ferromagnetic phase, the magnetization is favored to lie transverse to $\hat{x}$ for $q > 0$ (easy-plane) and along $\hat{x}$ for $q < 0$ (easy-axis).

This predicted phase diagram (for $q > 0$) was supported by studies of $F = 1$ spinor condensates of ^{87}Rb in the single spatial-mode regime, for which the condensate dimensions in all directions were comparable to the spin healing length, defined by $\xi_s = (8\pi\Delta an)^{-1/2}$ [13–15]. However, recent experiments on spatially extended spinor gases revealed variegated magnetization textures produced upon cooling unmagnetized spinor gases into the quantum degenerate regime [8]. Theoretical works examined whether such textures could be favored at equilibrium by the substantial magnetic dipolar interactions in the ^{87}Rb gas; however, while some inhomogeneous textures do appear energetically favored, or at least metastable, they are predicted to evince spin-density modulations only on much longer lengths scales than observed experimentally [16–21].

To resolve this discrepancy, we examine quantum-degenerate spinor Bose gases over evolution times of several seconds, much longer than previously [8]. We find that cooling non-degenerate gases with different initial spin compositions produces spin textures that differ strongly at short equilibration times, consistent with Ref. [8]. However, at least at small values of $|q| \lesssim h \times 10\,\text{Hz}$ and at the longest equilibration times [22], these textures do tend toward a common state characterized by large commonly magnetized regions and easy-plane/easy-axis magnetic anisotropy consistent with the predicted equilibrium phases of ferromagnetic spinor condensates with contact interactions. For larger values of $|q|$, the redistribution of Zeeman populations needed to yield the expected equilibrium states is dramatically slowed, preventing the appearance of a common state from differing initial populations.

For our experiments, we produce optically trapped, spin-polarized atomic gases in a manner similar to Ref. [23], with initial temperatures of 30 μK and initial trap frequencies of $(\omega_x, \omega_y, \omega_z) = 2\pi(220, 4150, 63)$ Hz in a focused, linearly polarized light beam with a wavelength of 1064 nm. We next prepare unmagnetized spin mixtures with fractional populations in the three Zeeman sublevels, $\zeta_{m_F}^{(th)}$ with $m_F = \{+1, 0, -1\}$, by the application of resonant $\pi/2$ rf pulses in the presence of a magnetic field gradient [8]. The spin mixtures are then cooled by lowering the optical trap depth over 2.4 s to a final trap depth of 1.5 μK and final trap frequencies of $(\omega_x, \omega_y, \omega_z) = 2\pi(25, 480, 7.3)$ Hz. We then allow for an equilibration period of up to $t = 4$ s, where $t = 0$ denotes the end of the ramp-down of the optical trap depth.

Throughout the evaporation and equilibration periods, a static magnetic field of $B = 267$ mG was applied along the $\hat{x}$ axis. The coordinate system is defined with respect to the optical dipole trap. The long axis of the trap (most weakly confined axis) is defined to be the $\hat{z}$ axis and the most tightly confined direction, parallel to gravity, is the $\hat{y}$ axis. The applied magnetic field causes the magnetization in the $\hat{y} - \hat{z}$ plane to precess with respect to the $\hat{x}$ axis at the Larmor frequency of $\Omega_L = 2\pi \times 187$ kHz. The magnetic field inhomogeneity is reduced to below 1 μG across the extent of the gas, resulting in a negligible spatial variation of less than 1 Hz in the Larmor precession frequency, as well as insignificant effects on the spin-mixing dynamics and spin textures reported here [12]. The field also produces a quadratic Zeeman energy shift $q_B = h(70\,\text{Hz}/\text{G}^2)B^2 \approx h \times 5$ Hz. In addition, the sample was exposed to a linearly polarized microwave-frequency magnetic field detuned by $\delta = \pm 2\pi \times 40$ kHz from the $|F = 1, m_F = 0\rangle$ to $|F = 2, m_F = 0\rangle$ hyperfine transition. The resulting ac Zeeman shift of $q_\mu = -\hbar\Omega^2/4\delta$ was used to tune the total quadratic shift $q = q_B + q_\mu$ by varying the Rabi frequency Ω and by choosing the sign of δ [24, 25].

The spinor gas was then measured either by time-of-flight analysis, through which we quantify the fractional Zeeman populations, $\zeta_{m_F}^{(c)}$, of the quasi-condensed portion of the gas, or by *in-situ* measurements of the vector magnetization. The term "quasi-condensed" is used since the quantum degenerate gas shows the bimodal *in-situ* spatial distribution and the time-of-flight momentum distribution characteristic of a trapped condensate, but lacks long-range phase coherence as evidenced by the inhomogeneous spin distributions we observed. We first discuss the time-of-flight measurements, which were performed on gases that were prepared initially with fractional Zeeman populations $\zeta_{m_F}^{(th)}$ of either 0, 1/4 or 1/3.

Evaporatively cooling such gases produces spinor condensates containing around 3×10^6 atoms, of which 30% are thermal, at $t = 0$, and around 1.2×10^6 atoms at $t = 4$ s. Assuming a conventional Thomas-Fermi distribution of condensed atoms within the optical trap, we determine the peak condensate densities to be $n_0 = 2.6 \times 10^{14}\,\text{cm}^{-3}$ at $t = 0$ and $1.8 \times 10^{14}\,\text{cm}^{-3}$ at $t = 4$ s, respectively. We note that bimodal time-of-flight distributions are observed already beginning at $t \simeq -50$ ms. At early times the spinor condensates are found to have fractional Zeeman populations identical to those of a non-degenerate gas from which the condensates form. Following that, spin-mixing collisions within the condensate cause the Zeeman populations to vary. For instance, starting with equal populations in the three Zeeman populations Fig. 1(a), the $\zeta_{\pm 1}^{(c)}$ population tends to decrease when the energy of the $|m_F = \pm 1\rangle$ states is raised ($q > 0$), and to increase when it is lowered ($q < 0$). Comparing measurements on samples with different initial spin compositions (Fig. 1(c)), we find that a common steady-state distribution among Zeeman levels is achieved within several

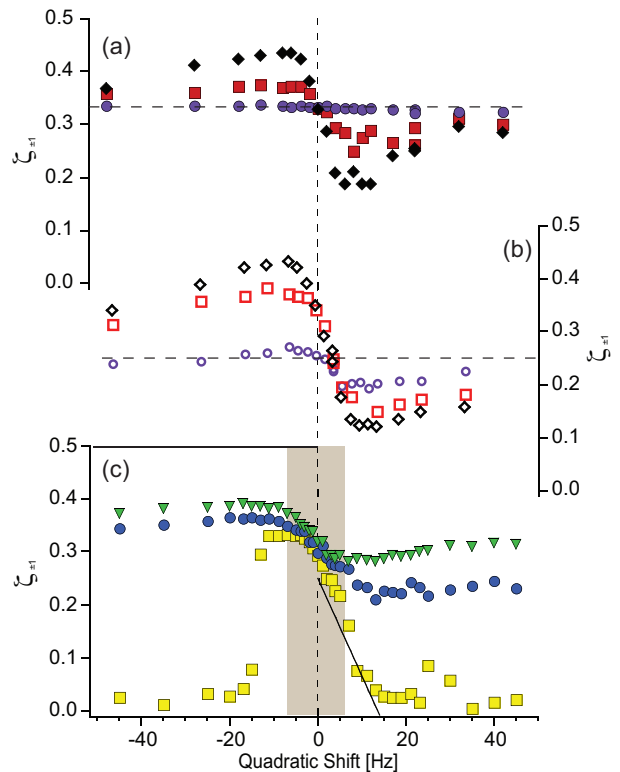seconds of equilibration, for $|q| \lesssim 10$ Hz.

FIG. 1: Condensate Zeeman populations, $\zeta_{\pm 1}^{(c)}$, during equilibration of unmagnetized spinor gases at variable q. Measurements at various evolution times $t = 200$ ms (purple circles), 1 s (red squares), and 3 s (black diamonds) are shown with initial $\zeta_{\pm 1}^{(th)} = 1/3$ (a) and 1/4 (b). In (c), Zeeman populations at $t = 2$ s are compared for initial $\zeta_{\pm 1}^{(th)} = 1/3$ (green triangles), 1/4 (blue circles), and 0 (yellow squares). For a narrow range $|q|/h \lesssim 5$ Hz (shaded), Zeeman populations evolve toward a common steady state within about 2 s, toward values qualitatively in accord with mean-field predictions (solid line in c) based on the spin-dependent contact interaction. Outside that range, initial population differences persist throughout the experimentally accessed equilibration times. Data are averages of 3 experimental runs.

We compare the measured Zeeman populations to the mean-field predictions for the uniform ground state of a ferromagnetic $F = 1$ spinor condensate [12]. For $q < 0$, the spin-dependent contact interaction is minimized by a fully magnetized condensate with magnetization aligned with the field axis $\hat{x}$. For our experiments, the total magnetization $\langle F_x \rangle = 0$ is conserved in the absence of dipolar relaxation. To satisfy this constraint, one might expect the condensate to be divided into domains of magnetization oriented along $\pm \hat{x}$, resulting in $\zeta_{\pm 1}^{(c)} = 0.5$. For $0 < q < 2|c_2|\langle n \rangle_y \simeq h \times 8$ Hz, where $\langle n \rangle_y = 1.85 \times 10^{14}\,\text{cm}^{-3}$ is the density averaged in the $\hat{y}$ direction after 2 s of equilibration, one expects that the condensate comprise transversely polarized spin domains in which $\zeta_{\pm 1}^{(c)}$ diminishes linearly from 0.25 to zero
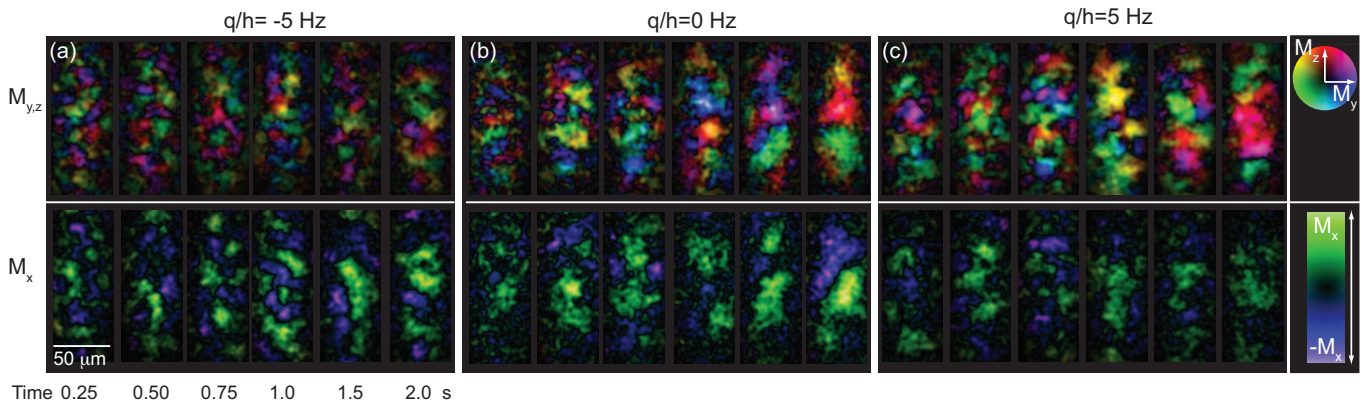
FIG. 2: Transverse (top) and longitudinal (bottom) magnetization after a variable evolution time at a quadratic shift of $q/h =$ -5 (a), 0 (b), and 5 (c) Hz for an initial spin mixture of $\zeta_{\pm 1}^{(th)} = 1/3$. The transverse magnetization is represented using the color scheme shown, where the hue indicates the magnetization orientation and the brightness its magnitude. The maximum brightness is set by a a fully polarized condensate at 2 s evolution time. The longitudinal magnetization is represented by the color bar. Textures form from initially small domains and then coarsen to where only a few domains span the entire condensate. The late-time images show a spin-space anisotropy; for positive q the transverse magnetization appears brighter while for negative q the opposite trend is observed.

[26]. At $q = 0$, fully magnetized domains of all spin orientations minimize the mean-field energy; one might therefore expect $\zeta_{\pm 1}^{(c)} = 1/3$. These predictions ignore the number and composition of domain boundaries, and agree qualitatively with our measurements at small $|q|$.

For larger values of $|q|$, the Zeeman populations do not reach a common steady state within the 4 s lifetimes of our trapped samples. For $q > 2|c_2|n_0$, the single-atom quadratic Zeeman shift is predicted to be sufficient to overcome the ferromagnetic spin-dependent contact interaction and lead to a condensate equilibrating purely in the $|m_F = 0\rangle$ state [12–14]. However, the condensates prepared with $\zeta_{\pm 1}^{(c)} \neq 0$ retain non-equilibrium Zeeman populations nearly equal to their initial values, with the rate of Zeeman-population transfer diminishing with increasing q. For $q < 0$, the single-atom quadratic Zeeman shift favors population in the $|m_F = \pm 1\rangle$ states. However, for $q/h \lesssim -20$ Hz, while condensates within non-zero initial values of $\zeta_{\pm 1}^{(th)}$ do evolve toward the presumed equilibrium distribution, a condensate prepared in the non-equilibrium $|m_F = 0\rangle$ Zeeman state shows almost no variation in its spin distribution. The extinction of spin-mixing dynamics at negative q for condensates in the $|m_F = 0\rangle$ states was observed previously [24].

The strong variation of spin-mixing dynamics with variations in q that are far smaller than the thermal energy ($k_B(50\,\mathrm{nK}) = h \times 1$ kHz) suggests that spin-mixing occurs primarily within the condensed fraction of the gas, with little influence of the non-condensed portion [27]. The variation of condensate spin-mixing dynamics with q has been studied in the single-mode regime [15, 28], showing that the amplitude of Zeeman-population oscillations diminishes at large quadratic shifts. This reduction in amplitude occurs once the energy difference introduced between the two-atom states coupled by spin

mixing becomes larger than the spin-mixing interaction strength ($|q| > 2|c_2|n$). The data here are in qualitative agreement with the spin mixing studies in the single mode regime. However, in these textures, spin mixing would occur within the strongly inhomogeneous regions between magnetized domains, which would complicate the dynamics of spin mixing oscillations and instabilities. Therefore, further experiments are needed to understand how this single-mode picture applies to the inhomogeneous spin textures studied here.

While the Zeeman-population measurements are indicative of equilibration dynamics, they do not reveal directly the spontaneous magnetization of the quantum degenerate gas nor do they characterize the spatial distribution of the condensate spin. To explore these properties, we employ magnetization-sensitive dispersive imaging. In contrast to previous work [29, 30], in which the magnetization was reconstructed from a series of images taken during Larmor precession, here we obtain a direct snapshot of the vector magnetization with just three images by applying spin-echo rf pulses between probes. Specifically, after a variable equilibration time, we apply the first imaging pulse, sending linear polarized probe light propagating along the $\hat{y}$ axis and measuring its optical rotation to resolve one transverse component of the column-integrated magnetization $\tilde{\mathbf{M}}(\rho)$ with the position vector ρ in the imaged $\hat{x}$-$\hat{z}$ plane. Following a delay τ_0 of about 50 μs, we apply a π pulse with a resonant rf magnetic field. We note that the entire sequence occurs within 500 μs, shorter than h/q. Thus, the quadratic Zeeman shift plays no role during the spin-echo sequence and the rf pulses effected simple rotations of the vector magnetization. In this sense, a π pulse rotates the spin vector by an angle π about a transverse axis selected by the phase of the rf signal [31, 32]. A second image, taken

after an additional delay $\tau = \tau_0 + \pi/2\Omega_L$, records the second component of the transverse magnetization. To measure the longitudinal magnetization component, we apply a properly timed π-$\pi/2$-π pulse sequence before taking a third image. This spin-echo imaging sequence functions reliably even in the presence of $> 2\pi \times 10$ kHz variations in Ω_L between experimental runs. The imaging light is detunned 400 MHz above the $F = 1 \rightarrow F' = 2$ $D1$ transition with a pulse duration of 300 ns, much shorter than the one quarter of the Larmor precession period to avoid averaging of the magnetization signal. By using far few images than in our previous technique, the spin-echo imaging method should allow for higher resolution images (on a limited-area camera) or repeated imaging of spinor gases.

The temporal evolution of spin textures produced upon cooling thermal mixtures with $\zeta_{\pm 1}^{(th)} = 1/3$ is shown in Fig. 2 for three different settings of q. Within several hundred milliseconds, a highly corrugated spin texture develops within the condensate consisting of small domains with magnetization orientations distributed isotropically. The domains have a typical diameter of about 10 microns, in agreement with previous observations [8], although the textures in the present experiment do not show a preferred direction for spatial modulation of the magnetization in the $\hat{x}$-$\hat{z}$ plane.

The next few seconds of equilibration lead to distinct changes in both the composition and the spatial arrangement of the spin textures. The magnetization develops a q-dependent spin-space anisotropy visible in the contrasting magnetization amplitudes for different quadratic shifts (Fig. 2). Also evident is the development of larger domains of common magnetization. At early times the magnetization map consists of many randomly oriented spin domains and subsequently within 2-3 s, the texture contains just a few domains, spanning the entire width of the condensate.

To characterize these changes we consider the dimensionless correlation functions of the i component of the magnetization vector, given as

$$G_i(\delta\rho) = \frac{\sum_\rho \tilde{M}_i(\rho + \delta\rho)\tilde{M}_i(\rho)}{\mu^2 \sum_\rho \tilde{n}(\rho + \delta\rho)\cdot\tilde{n}(\rho)}, \qquad (1)$$

with μ being the atomic magnetic moment. This correlation function is evaluated over the central 35×85 μm^2 area of the condensate.

Setting $\delta\rho = 0$, we obtain the variance of the longitudinal magnetization $G_L(0) = G_x(0)$, and also the average of the transverse magnetization $G_T(0) = (G_y(0) + G_z(0))/2$ [33]. For a fully magnetized gas $G_L(0) + 2 \times G_T(0) = 1$. As shown in Fig. 3 (inset) for an initially unpolarized gas with an initial spin composition of $\zeta_{\pm 1}^{(th)} = 1/3$, magnetization at early equilibration times ($t \lesssim 700$ ms) develops with equal variance in the longitudinal and transverse orientations. Thereafter, within 2 s, the sum of the variances become consistent with unity and the magnetization develops a spin-space anisotropy: easy-plane

or easy-axis anisotropy seen from the enhanced transverse or longitudinal magnetization, for $q > 0$ or $q < 0$, respectively (Fig. 3). At $q = 0$, the magnetization orientation remains isotropic. Both the q-dependence and also the 1-2 s timescale for development of the spin-space anisotropy are consistent with the Zeeman-population measurements discussed above.

A second trend in the evolution of these spin textures is the development of ever-larger domains of common magnetization. The coarsening dynamics are characterized by measuring the area A of the central region of positive vector magnetization correlations, obtained by summing $G_i(\delta\rho)$ over all spin components. The typical domain length $l = \sqrt{4A/\pi}$ grows continuously from its initial value of about 10 μm to a final value $l \simeq 40$ μm over the 3 s equilibration time examined in our measurements (Fig. 4).

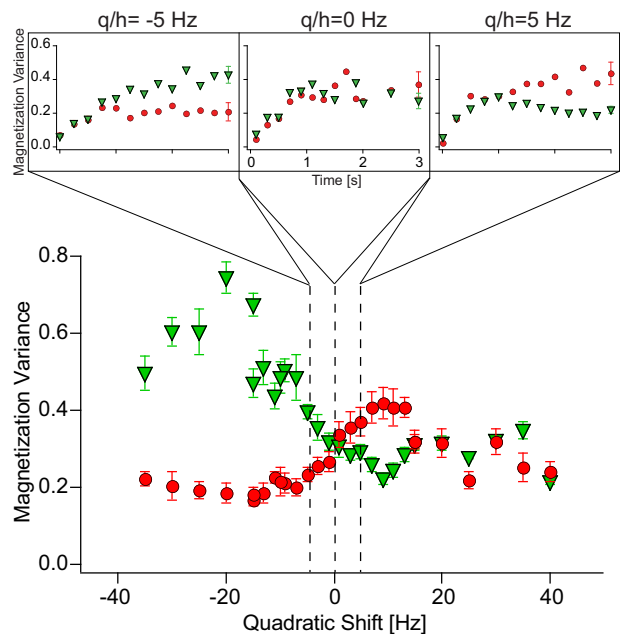

FIG. 3: The magnetization variance versus q for $\zeta_{\pm 1}^{(th)} = 1/3$ at t=2 s for transverse magnetization $G_T(0)$(red circles) and longitudinal magnetization $G_L(0)$ (green triangles). For $q = 0$ the longitudinal and transverse magnetization variances are equal, showing no preference in spin orientation (isotropic), while for $q > 0$ ($q < 0$), the data show a preference for transverse (longitudinal) magnetization, seen in the larger transverse (longitudinal) magnetization variance (easy plane/easy axis). (Inset) Temporal evolution of the transverse ($G_T(0)$, red circles) and longitudinal ($G_L(0)$, green diamonds) magnetization variance, evaluated within the central regions of spin textures produced from $\zeta_{\pm 1}^{(th)} = 1/3$ spin mixtures at $q/h = -5$ Hz (left), 0 Hz (middle) and 5 Hz (right). At early equilibration times, $t \lesssim 700$ ms, the magnetization has equal variance in the longitudinal and transverse orientations. Within 1-2 s, a clear preference for longitudinal orientation at $q > 0$ (middle), while for $q = 0$ the spin distribution remains isotropic. Data are the average of 6 experimental repetitions, and error bars are the standard deviation of the data.

Phase-ordering kinetics from an initially disordered state have been studied in numerous systems [34]. Coarsening dynamics is often found to yield a self-similar domain pattern with a characteristic length scale that evolves temporally as a power law $l(t) \propto t^b$, where the exponent b depends on the order parameter of the system. Adapting such classical theories to the coarsening of spin textures in a spinor condensate [35, 36], one expects the conserved order parameter to vary effectively from a scalar order parameter (easy axis), for which $b = 1/3$, to a vector order parameter (easy plane/isotropic), for which $b = 1/4$, according to the quadratic Zeeman shift [37, 38]. For $q > 0$ we expect similar domain coarsening dynamics to the behavior observed for $q = 0$, whereas for $q < 0$, the rate of domain growth is expected to be slightly faster.

The observed coarsening dynamics and the ability to tune the order parameter in a spinor condensate could enable a quantitative comparison with theories of phase-ordering kinetics. Typically, such theories stress the use of large systems where the smallest observed length scale is orders of magnitude smaller than the sample size, and finite-size effects can be safely ignored [39, 40]. However, in the present experiment, the initial domain length of $10\,\mu$m is on the order of the transverse width of the gas, and simple scaling behavior is therefore unlikely. Future experiments with spinor gases of larger spatial extents may enable more quantitative comparison with theory.
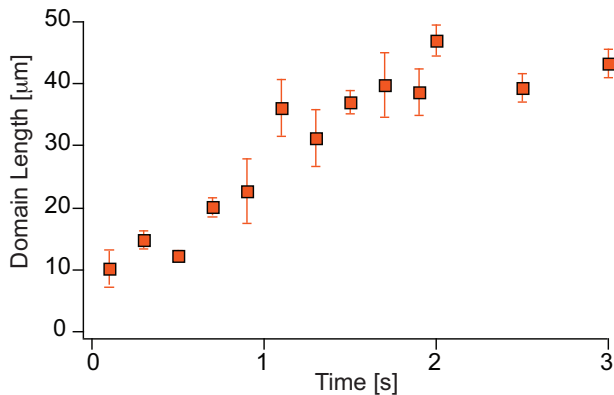

FIG. 4: Temporal evolution of domain length after variable evolution time at a quadratic shift of 0 Hz for an $\zeta_{\pm1}^{th} = 1/3$ mixture. The domain length, as defined in the text, grows smoothly as a function of the evolution time, with domains of about $10\,\mu$m to final values of $40\,\mu$m within 2 s.

In conclusion, we observe four temporal trends: a redistribution of Zeeman populations, the development of magnetization from the initially unmagnetized gas, the development of a spin-space anisotropy, and the coarsening of spin domains. For small $|q|$, all of these trends occur on a similar 1-2 s timescale, allowing the system to reach a common final state, independent of the initial spin composition. For larger $|q|$, equilibrium is not reached within the accessible experimental timescales. The timescale for spin mixing dynamics is set by the spin-dependent interaction energy, $2|c_2|n \approx h \times 8$ Hz, resulting in spin mixing timescales of $\tau_{sm} = h/(2|c_2|n)$, far shorter than the observed seconds-long equilibration times. It remains unclear what determines the dynamical timescales for each of the observed processes.

[1] I. Bloch, J. Dalibard, and W. Zwerger, Reviews of Modern Physics **80**, 885 (2008).

[2] T. Kinoshita, T. Wenger, and D. S. Weiss, Nature **440**, 900 (2006).

[3] C.-L. Hung, X. Zhang, N. Gemelke, and C. Chin, Physical Review Letters **104**, 160403 (2010).

[4] S. S. Natu, K. R. A. Hazzard, and E. J. Mueller, Physical Review Letters **106**, 125301 (2011).

[5] L. Sadler, J. Higbie, S. Leslie, M. Vengalattore, and D. Stamper-Kurn, Nature **443**, 312 (2006).

[6] M. Scherer, B. Lucke, G. Gebreyesus, O. Topic, F. Deuretzbacher, W. Ertmer, L. Santos, J. J. Arlt, and C. Klempt, Physical Review Letters **105** (2010).

[7] M. Vengalattore, S. Leslie, J. Guzman, and D. Stamper-

Kurn, Physical Review Letters **100**, 170403 (2008).

[8] M. Vengalattore, J. Guzman, S. R. Leslie, F. Serwane, and D. M. Stamper-Kurn, Physical Review A **81**, 053612 (2010).

[9] T.-L. Ho, Physical Review Letters **81**, 742 (1998).

[10] T. Ohmi and K. Machida, Journal of the Physical Society of Japan **67**, 1822 (1998).

[11] C. Law, H. Pu, and N. Bigelow, Physical Review Letters **81**, 5257 (1998).

[12] J. Stenger, S. Inouye, D. Stamper-Kurn, H.-J. Miesner, A. Chikkatur, and W. Ketterle, Nature **396**, 345 (1998).

[13] H. Schmaljohann, M. Erhard, J. Kronjäger, M. Kottke, S. v. Staa, L. Cacciapuoti, J. J. Arlt, K. Bongs, and K. Sengstock, Physical Review Letters **92**, 040402 (2004).

[14] M.-S. Chang, C. D. Hamley, M. D. Barrett, J. A. Sauer, K. M. Fortier, W. Zhang, L. You, and M. S. Chapman, Physical Review Letters **92**, 140403 (2004).

[15] M.-S. Chang, Q. Qin, W. Zhang, L. You, and M. Chapman, Nature Physics **1**, 111 (2005).

[16] M. Takahashi, S. Ghosh, T. Mizushima, and K. Machida, Physical Review Letters **98**, 260403 (2007).

[17] R. W. Cherng and E. Demler, Physical Review Letters **103**, 185301 (2009).

[18] J. A. Kjall, A. M. Essin, and J. E. Moore, Physical Review B **80**, 224502 (2009).

[19] Y. Kawaguchi, H. Saito, K. Kudo, and M. Ueda, Physical Review A **82**, 043627 (2010).

[20] J. A. Zhang and T. L. Ho, Journal of Low Temperature Physics **161**, 325 (2010).

[21] J. A. M. Huhtamäki, M. Takahashi, T. P. Simula, T. Mizushima, and K. Machida, Physical Review A **81**, 063623 (2010).

[22] R. Barnett, A. Polkovnikov, and M. Vengalattore, Phys. Rev. A **84**, 023606 (2011).

[23] Y. J. Lin, A. R. Perry, R. L. Compton, I. B. Spielman, and J. V. Porto, Physical Review A **79**, 063631 (2009).

[24] S. Leslie, J. Guzman, M. Vengalattore, J. D. Sau, M. L. Cohen, and D. Stamper-Kurn, Physical Review A (Atomic, Molecular, and Optical Physics) **79**, 043631 (2009).

[25] F. Gerbier, A. Widera, S. Folling, O. Mandel, and I. Bloch, Physical Review A **73**, 041602 (2006).

[26] From a mean-field treatment of a homogeneous ferromagnetic spinor condensate with uniform density n_0 we obtain $\zeta_{\pm 1} = (2 - \epsilon)/8$ with $\epsilon = -q/c_n n_0$ in the range $0 < \epsilon \leq 2$.

[27] The experiments presented here were conducted with an initial fraction of thermal atoms that is approximately 0.30 of the total number of atoms detected. Other experiments were conducted at an initially lower fraction of thermal atoms, 0.12, which yielded similar results, where the thermal fraction showed no variation with quadratic shift, in contrast to the condensed portion.

[28] J. Kronjager, C. Becker, P. Navez, K. Bongs, and K. Sengstock, Physical Review Letters **97**, 110404 (2006).

[29] J. Higbie, L. Sadler, S. Inouye, A. P. Chikkatur, S. R. Leslie, K. L. Moore, V. Savalli, and D. M. Stamper-Kurn, Physical Review Letters **95**, 050401 (2005).

[30] M. Vengalattore, J. M. Higbie, S. R. Leslie, J. Guzman, L. E. Sadler, and D. M. Stamper-Kurn, Physical Review Letters **98**, 200801 (2007).

[31] J. Higbie, Ph.D. thesis, University of California, Berkeley (2005).

[32] J. Kronjager, C. Becker, M. Brinkmann, R. Walser, P. Navez, K. Bongs, and K. Sengstock, Physical Review A **72**, 063619 (2005).

[33] In practice, to lower the noise in variance measurements, we set $G_{L,T}(0)$ equal to the averages of the respective magnetization correlation functions over a $3.5 \times 3.5 \, \mu m^2$ region centered at $\delta\rho = 0$.

[34] A. J. Bray, Advances in Physics **51**, 481 (2002).

[35] N. Keekwon, K. Bongsoo, and S. J. Lee, Journal of Statistical Mechanics: Theory and Experiment (2011).

[36] C. Josserand and S. Rica, Phys. Rev. Lett. **78**, 1215 (1997).

[37] M. Siegert and M. Rao, Physical Review Letters **70**, 1956 (1993).

[38] J. F. Marko and G. T. Barkema, Physical Review E **52**, 2522 (1995).

[39] S. Majumder and S. K. Das, Phys. Rev. E **84**, 021110 (2011).

[40] S. Mukerjee, C. Xu, and J. E. Moore, Phys. Rev. B **76**, 104519 (2007).